Simple Model of a Piano Soundboard

N. Giordano

Department of Physics, 1396 Physics Building, Purdue University, West Lafayette, IN 47907-1396

Abstract

The vibrational properties of a simple finite element model of a piano soundboard are considered. Our main focus is on the behavior of the mechanical impedance in the musically important frequency range $\sim 50 - 10^4$ Hz. The model includes the effects of elastic anisotropy and the ribs. It is argued that the ribs are an essential ingredient for producing the behavior of the impedance which is observed experimentally.

I. INTRODUCTION

The problem of modeling a piano would at first glance seem to be straightforward. One needs to consider the vibrations of a flexible string which is held fixed at one end and is attached to a flexible plate, the soundboard, at the other. The vibrations of the soundboard lead in turn to sound production. However, while the physics of vibrating strings and plates is generally well understood, there are numerous complications, such as the effects of string stiffness, the precise nature of the connection of the string to the soundboard (which leads to coupling of the different modes of polarization of the vibrations of the string), the nonlinear behavior of the hammers, and the complicated shape of the soundboard. Because of such difficulties, the current state of the art in piano modeling does not produce a convincing piano sound; nevertheless, progress has been made toward this goal in recent years. For example, Chaigne and Askenfelt [1,2] have treated the hammer-string interaction in detail, along with the effect of string stiffness, and have obtained good agreement with certain aspects of the experimental observations. However, their calculations do not include coupling to the soundboard, assuming instead that both ends of the string are held perfectly rigid. Energy loss from the string is then accounted for through the use of ad-hoc frequency dependent damping terms which are added to the equation of motion for the string. This approach has serious limitations, as it precludes, for example, any treatment of coupling between strings.

One would clearly like to model the soundboard in a quantitative manner, and while progress along these lines has been made for the piano [3–7], the guitar [8–11], and the violin [12], much remains to be done in this area. The purpose of the present paper is to discuss a simple model of a piano soundboard, and compare its properties with those observed for real soundboards. The model that we ultimately arrive at will be an extremely simple one consisting of a square board, with the grain oriented parallel to one edge of the board and with ribs running perpendicular to the direction of the grain. This is certainly not intended to be a "completely realistic" model of a real soundboard, but rather as an aid in understanding those aspects of the board which are essential for its proper acoustical performance. One of

the goals of this work is to construct a real time model (as opposed to one which operates in the frequency domain) which can be used in conjunction with piano string simulations like those of Ref. [1]. We will also attempt to identify how different properties of the model, such as elastic anisotropy and the presence of ribs, affect the behavior. Our calculations and arguments are not profound, but we believe that they bring out some important points that we have not seen discussed previously in the literature.

II. EXPERIMENTAL FACTS AND SOME GENERAL OBSERVATIONS

Figure 1 shows, in schematic form, results for the magnitude of the mechanical impedance, $\mid Z \mid \equiv F_0/v_0$, as a function of frequency from experiments with an upright piano [13]. Here F_0 is the amplitude of an applied force, which is a sinusoidal function of time with frequency f. This force is applied to a particular point on the board (as will be specified below), and v_0 is the steady state amplitude of the velocity of the board at the same location, also at frequency f. While our sketch shows the impedance as a fairly smooth function of frequency, the effects of soundboard resonances are clearly seen in the measured data, and several such resonances are shown semi-quantitatively in Fig. 1. We also show the measured sound power level as a function of frequency, as recorded with a microphone a short distance from the soundboard. Here the board was driven harmonically, and F_0 was adjusted to obtain the same value of v_0 at all frequencies. The bottom plot in Fig. 1 shows the phase of the steady state soundboard velocity relative to the drive force. We will be comparing all of the results in Fig. 1 with our model calculations below. The results for the impedance in Fig. 1 are the main experimental facts that we wish to understand and explain. It is worthwhile at this point to consider precisely which features of the experimental results are musically important. Let us discuss the frequency ranges < 100, $100 - 10^3$, and $10^3 - 10^4$ Hz separately.

At frequencies which are below the fundamental soundboard mode, $\mid Z \mid$ increases as f is lowered. For the particular soundboard considered in Ref. [13] this mode occurred

near 100 Hz, and that seems to be a typical value [3,5,15]. The sound generation efficiency in this range will generally be very low, since the size of the source differs greatly from the wavelength of the radiation; this low efficiency is also evident from the measurements (Fig. 1). In addition, the fundamental frequency for most strings is above this range, so they do not drive the soundboard at these frequencies. The behavior of $\mid Z \mid$ in this range should also be relatively easy to model, since as we will see below it depends mainly on having the fundamental soundboard mode at the proper frequency.

In the range $100 - 10^3$ Hz one finds that $\mid Z \mid$ exhibits a number of resonances, and it varies around an "average" value which is near 10^3 kg/s. This average value depends somewhat (by a factor of ~ 2) on the position at which one measures the impedance (i.e., where the force is applied). The resonant structure in $\mid Z \mid$ arises from the many soundboard modes which occur above the fundamental. As is well appreciated [13,16,17], it is important that this resonant structure not be too pronounced, as it could lead to an uneven response as one moves across the keyboard. The difference between the peaks and valleys in $\mid Z \mid$, and the widths of these resonances, will depend on the magnitude of the loss. We should also note that the resonant structure in $\mid Z \mid$ varies with location on the soundboard [13]. It seems likely that good pianos are designed to avoid positioning a string at locations where it can strongly excite a resonance corresponding to its particular frequency. A second important feature of the impedance in this frequency range is its overall value. This is important with regards to the strength with which a string couples to the soundboard. The efficiency with which energy is transmitted from the string to the soundboard is governed by the impedance mismatch between the two. This is of great importance, since it determines the rate at which a string vibration decays and hence the duration of the sound. It seems likely that the value of $\mid Z \mid$ seen in Fig. 1, which has also been reported elsewhere [18], gives the "proper" amount of coupling and hence the proper decay rate. Here the term "proper" means that the coupling and decay rate yield sounds which are musically pleasing to a listener. Thus, it is also the behavior observed in concert-quality pianos. A successful soundboard model should therefore give an impedance near 10^3 kg/s in this middle frequency range. This

conclusion has also been reached by Conklin [19].

Lastly we consider the high frequency range $10^3 - 10^4$ Hz. Here the resonant structure is much less pronounced than at lower frequencies, and there is a monotonic decrease in $\mid Z \mid$ from a value near 10^3 kg/s at $\sim 10^3$ Hz to ~ 30 kg/s at 10^4 Hz [20]. We believe that this fall off is important for the following reason. The string impedance varies somewhat across the keyboard, from ~ 10 kg/s in the bass to ~ 5 kg/s in the treble [13], and is always much less than the impedance of the board. We have already noted that the string-soundboard mismatch determines how fast a string vibration will decay. It is well known that this decay time becomes shorter as one moves from strings in the bass to those in the treble, and also that for a given string the decay time becomes shorter as one goes to higher frequencies (higher order partials) [21,22]. Theoretically we know that the decay time will become shorter as the impedance mismatch is reduced. Hence, one way to account for this behavior of the decay time is to assume that Z of the soundboard decreases at high frequencies so as to reduce the mismatch with the string. The argument then is that the decrease of the impedance of the soundboard observed at high frequencies is important for obtaining the proper frequency dependence of the decay rate. Given that this is also observed in the experiments of Ref. [13], the implication is that a successful soundboard model must exhibit this behavior. (However, there may be other sides to this argument; we will return to this point below [23].)

Let us now consider what is perhaps the simplest possible model of a soundboard, and compare its properties to those we desire. The board is modeled as a single mass connected to a rigid support via a spring, with a damping term to account for sound generation and losses inherent in the board itself. A plausible equation of motion is then

$$m\frac{d^2z}{dt^2} \;=\; -Kz - R\frac{dz}{dt} + F \;, \tag{1}$$

where z is the displacement (not to be confused with Z) and m the mass of the soundboard, K is the spring constant, F is an applied force due to the string, and R determines the magnitude of the damping. The properties of this simple "single oscillator" model of the

board can be readily calculated. If we assume a driving force of the form $F = F_0 e^{i\omega t}$, the steady state velocity of the board is given by [16]

$$v \;=\; \frac{F_0 e^{i\omega t}}{R + i(\omega m - K/\omega)} \;. \tag{2}$$

The mechanical impedance is $Z \equiv F/v$. From (2) we find that above the resonant frequency of the board ($\omega_0 = \sqrt{K/m}$), the imaginary part of Z increases with frequency, while its real part is constant. Since the energy loss rate is equal to $\mathrm{Re}(Fv) = \mathrm{Re}(F^2/Z)$ (here Re() denotes the real part of an expression), one sees that the loss will decrease rapidly at frequencies above ω_0. This high frequency response is "mass dominated," and it is seen to be property of any mass-spring system at frequencies above all of the resonant frequencies of the system.

For a real piano soundboard the fundamental resonance is typically near 100 Hz, and the resonant frequency of the model (1) can always be adjusted to give this value for ω_0. The other parameters in the model can then be chosen to give an overall value of $\mid Z \mid$ near the desired 10^3 kg/s. However, the single oscillator model exhibits an impedance which increases above its resonant frequency, so it will *always* yield a string decay rate that decreases with increasing frequency. If a real soundboard were to behave in this fashion, only the high frequency partials would remain after a short time, yielding an unpleasant tone. This is, of course, contrary to observations [21,22,16].

The difficulty with the single oscillator model (1) can be restated as follows. The fundamental (i.e., lowest frequency) mode of the soundboard must be near 100 Hz, so as to match the fundamental mode of real soundboards. However, the behavior at frequencies up to at least 10^4 Hz must not be "mass-like." The only way this can happen is for the soundboard to have a distribution of resonant modes over this range. It must therefore be treated as a spatially extended system, which should not come as a surprise. A model with only one or a small number of oscillators must therefore be inadequate for a treatment of the behavior at frequencies above a few hundred Hz. This leads us to consider a spatially extended model in the next section.

We should note that a model which employs (1), or something like it, to describe each of a small number of oscillators may be useful in dealing with the low frequency behavior. Models of this kind for a guitar soundboard have been used successfully in the appropriate low frequency range [9–11].

III. ISOTROPIC BOARD

There have been several previous discussions of piano soundboards, from both experimental and theoretical points of view [24]. Among the experiments have been studies of the detailed vibrational modes, the eigenfrequencies and eigenvectors, exhibited by specific soundboards. This work has usually focussed on the lowest few modes, typically below a few hundred Hz [4,5,13,15,25,19], since at higher frequencies the relative separation of the modes becomes small and their displacement patterns (eigenvectors) become more complicated, making the modes difficult to distinguish individually. Theoretically it has been shown that these low frequency vibrations can be understood quantitatively in terms of models based on vibrating plates, provided that one includes the ribs and bridges. One interesting observation [5] is that the vibrations of the rim must also be included in order to accurately account for the modal frequencies and eigenvectors.

Since our ultimate goal is to produce a soundboard model which can be used for time domain simulations of the entire string-soundboard-sound system, it is necessary to push the modeling to higher frequencies. We will therefore attempt to focus instead on the *general* features of the model which are needed to obtain the behavior which was discussed in the previous section. Our aim is *not* to construct a model which accurately accounts in detail for the vibrational modes of any real soundboard. Rather, we want to understand what ingredients are necessary in order for a model to exhibit the *general* behavior observed for the impedance as a function of frequency as sketched in Fig. 1. Of course, at some point in the future one may want to design a model which does both.

In this and the next two sections we will consider several models of vibrating plates.

The first and simplest model we consider is a homogeneous, isotropic plate. The equation of motion is then [16,26]

$$\rho h \frac{\partial^2 z}{\partial t^2} = -D\nabla^4 z \ , \tag{3}$$

where z is the displacement of the plate in the direction perpendicular to its plane, h its thickness, ρ its density, and D is the rigidity which is given by

$$D = \frac{h^3 E}{12(1-\nu^2)} \ . \tag{4}$$

Here E is Young's modulus, and ν is Poisson's ratio. We consider a thin plate with vibrations only along z, so $\nabla^2 = \frac{\partial^2}{\partial x^2} + \frac{\partial^2}{\partial y^2}$. This model assumes that the plate is elastically isotropic, while a real soundboard certainly is not. We will add anisotropy to the model in the next section, but it is useful to consider the isotropic case first.

While the equation of motion (3) can be solved exactly (for simple plate geometries), we will soon be considering more complicated models for which such solutions are not readily available [27,28]. We will therefore consider the finite difference version of (3) in which the plate is divided into N^2 elements, each of area $(\Delta x)^2$ and mass $\rho h(\Delta x)^2$, arranged on a square grid. The displacement of the plate as a function of position and time then becomes $z(x,y,t) \to z(i,j,n)$, where i, j, and n are integers with $x = i\Delta x$, $y = j\Delta x$ (for simplicity we take the grid size to be the same in the x and y directions), and $t = n\Delta t$. We then write the derivatives in (3) in the usual finite difference forms [29], and rearrange to obtain $z(i,j,n+1)$, the displacement at time step $n+1$, in terms of the displacement at earlier times. The result is

$$\begin{aligned} z(i,j,n+1) = {} & a_1 z(i,j,n) + a_2 z(i,j,n-1) \\ & + a_3 \left[z(i+2,j,n) - 4z(i+1,j,n) + 6z(i,j,n) - 4z(i-1,j,n) + z(i-2,j,n) \right] \\ & + a_4 \left[z(i,j+2,n) - 4z(i,j+1,n) + 6z(i,j,n) - 4z(i,j-1,n) + z(i,j-2,n) \right] \\ & + a_5 \left[z(i+1,j+1,n) + z(i+1,j-1,n) + z(i-1,j+1,n) + z(i-1,j-1,n) \right. \\ & \quad \left. -2z(i+1,j,n) - 2z(i-1,j,n) - 2z(i,j+1,n) - 2z(i,j-1,n) + 4z(i,j,n) \right] \\ & + a_6 F(i,j,n) \ , \end{aligned} \tag{5}$$

where we have grouped the terms according to their origin (this grouping will also be convenient when we discuss generalizations of the model below). The coefficients a_i are given by

$$
\begin{aligned}
a_1 &= \frac{2}{1+\beta} \\
a_2 &= \frac{-1+\beta}{1+\beta} \\
a_3 &= \frac{-D(\Delta t)^2}{\rho h(\Delta x)^4} \\
a_4 &= \frac{-D(\Delta t)^2}{\rho h(\Delta x)^4} \\
a_5 &= \frac{-2D(\Delta t)^2}{\rho h(\Delta x)^4} \\
a_6 &= \frac{(\Delta t)^2}{\rho h(\Delta x)^2} \ ,
\end{aligned}
\tag{6}
$$

with

$$
\beta = \frac{R\Delta t}{2\rho h} \ . \tag{7}
$$

The parameter β is a measure of the dissipation, as we have now generalized the model (3) slightly by adding both a driving force and damping. The force applied to element (i,j) at time step n is $F(i,j,n)$, and is allowed to be a function of position. The damping force on a mass element is assumed to be of the form $-Rv(i,j)(\Delta x)^2$, where $v(i,j)$ is its velocity and R is a parameter which sets the scale for the damping [compare with (1)].

For the calculations we began with $z(i,j,0) = 0$ for all i and j; i.e., an undisplaced board at time $t = 0$. A force $F_0 \sin(2\pi f t)$ was then applied at only one grid site so as to have the same situation as in measurements of the driving point impedance. The displacement of the board as a function of time was then computed iteratively using (5). Here and for all of the calculations described below, clamped boundary conditions were employed at the edges of the board so as to approximate a soundboard clamped to a rim. Our main concern will be with the behavior at frequencies well above those of the lowest modes, so we expect that similar results would be found with simply supported or hinged boundaries (the modes at

the lowest frequencies are generally the ones affected most by the boundary conditions). At each frequency the simulation was run for several (usually 10 or more) periods of the drive frequency to allow the system to reach a steady state, before calculating the amplitude of the velocity at the driving point (used to calculate $\mid Z \mid$), the phase of this velocity relative to F, and other quantities [30].

Some typical results for an isotropic board are given in Fig. 2 where we show the driving point impedance as a function of frequency for two choices of the Young's modulus. Here we consider only $\mid Z \mid$; phase information is also available, but we will not consider it until we have arrived at a model which yields acceptable results for $\mid Z \mid$ (which will not come in this section). $\mid Z \mid$ is the ratio of the amplitude of the force at a particular location to the amplitude of the velocity of the board at the same location. Note that we chose a driving point somewhat off center (see the caption of Fig. 2), to avoid the nodal lines of any especially symmetric modes. We have assumed a square soundboard 1 m across (as a *very* rough approximation to an upright piano), with a uniform thickness of 1 cm and a density of 0.5 g/cm^3 (typical of the spruce used for soundboards). We have taken the Young's modulus to be $E = 1 \times 10^{10}$ N/m^2 in one of the calculations, and 4×10^8 N/m^2 in the other. In both cases we used a Poisson's ratio of $\nu = 0.3$. Since wood is anisotropic it has different values of these parameters along, as compared to across, the grain. These are typical along-the-grain and across-the-grain values of E for quarter cut spruce (this is the type of cut used for soundboards [31,19]). As our model assumes isotropy, the best we can do at this point is consider the behavior for these two extremal values of E. A quantity which is more difficult to estimate is the loss parameter, R. Fortunately it is not as important as the others in determining the overall behavior, and especially the average magnitude, of $\mid Z \mid$. Its main role at this point is to remove singularities at the resonances and smooth out the response. Since we are interested in only the general behavior and not in the details of specific resonances, the rather coarse frequency steps used in the calculations of Fig. 2 were sufficient. The solid lines in the figure simply connect the calculated values, but the overall behavior of $\mid Z \mid$ should be clear.

We first consider the behavior for the stiffer board (the larger value of E). The lowest resonant mode in this case occurs near 80 Hz; this resonance is signaled by the dip in $\mid Z \mid$ at this frequency. Additional calculations, which are not shown here, verified the location of the resonance and also its eigenvector. The resonant frequency is in agreement with the exact result for the lowest mode with these boundary conditions, which is ~ 77.5 Hz [16]. Below this frequency $\mid Z \mid$ increases as f is reduced, as expected for the stiffness dominated regime of an oscillator [16]. At higher frequencies $\mid Z \mid$ fluctuates considerably, as one passes through many resonances. The relative magnitudes of these fluctuations and the quality factors of the resonances are functions of the loss factor R, and we have chosen its value to give results which roughly match those observed for real soundboards [13]. Comparing the calculated $\mid Z \mid$ with the observations in Fig. 1 we note several differences. We begin with the result for $E = 1 \times 10^{10}$ N/m^2, the stiffer of the two cases considered. First, the average value of $\mid Z \mid$ calculated at intermediate frequencies, $100 - 10^3$ Hz, is close to the experimentally measured value of 1×10^3 kg/s. However, at frequencies in the range $10^3 - 10^4$ Hz, the calculated $\mid Z \mid$ is too high and does not fall sufficiently as frequency is increased. Indeed, it is approximately independent of frequency from below 100 to 10^4 Hz. For the softer board ($E = 4 \times 10^8$ N/m^2) the impedance is too low at low frequencies by nearly a factor of 10, and also does not fall as rapidly at high frequencies as observed in the measurements, Fig. 1. The trends seen in going from the stiff to the soft board make it clear that no choice of E for an isotropic board will yield the behavior observed for the impedance of real soundboards.

Perhaps most troubling is the fact that the calculated impedance varies little with frequency, especially since we have argued that this is crucial feature of the behavior of real soundboards. That this result should be found in the calculation can be understood as follows. The "average" value of Z will depend on the density of modes in a given frequency range. For a vibrating plate at frequencies above the lowest few modes, the density of modes is a constant [17,16], so it is not surprising to find that $\mid Z \mid$ is also approximately constant, as we have observed. Indeed, analytic results confirm that $\mid Z \mid$ for an infinite board is a constant for this model [32].

Since we want our model to exhibit an impedance which decreases substantially above 10^3 Hz, let us consider how one might obtain such behavior. In order to reduce $\mid Z \mid$ the velocity of the board must be larger for a given amplitude of the force; i.e., the board must be effectively softer. One way to make the board softer is to reduce the Young's modulus. However, as we have seen from Fig. 2, simply reducing E will not take us to this goal. This is not surprising in view of the density of modes argument just given. This leads us to consider a somewhat more realistic model, a board with elastic anisotropy, which will be described in the next section.

IV. ANISOTROPIC BOARD

Real soundboards are generally made of quarter cut wood [31,19], so that elastically they are highly anisotropic. In terms of the Young's modulus the anisotropy is typically a factor of ~ 10 or more. We therefore consider an anisotropic model with different elastic constants in the x and y directions. We will imagine that the grain of the soundboard runs parallel to the x axis, so that the "soft" direction is along y [33]. The equation of motion for such a board, which is generally termed "orthotropic," is [5,34]

$$\rho h \frac{\partial^2 z}{\partial t^2} = -D_x \frac{\partial^4 z}{\partial x^4} - \left(D_x \nu_y + D_y \nu_x + 4 D_{xy}\right) \frac{\partial^4 z}{\partial x^2 \partial y^2} - D_y \frac{\partial^4 z}{\partial y^4} \ , \tag{8}$$

where the rigidity factors are

$$\begin{aligned} D_x &= \frac{h^3 E_x}{12(1-\nu_x \nu_y)} \\ D_y &= \frac{h^3 E_y}{12(1-\nu_x \nu_y)} \\ D_{xy} &= \frac{h^3 G_{xy}}{12} \ . \end{aligned} \tag{9}$$

Here E_x and ν_x are the Young's modulus and Poisson's ratio for the x direction, etc., for y, and G_{xy} is the shear modulus. Converting to a set of difference equations, the form is the same as (5) and the coefficients become

$$
\begin{aligned}
a_1 &= \frac{2}{1+\beta} \\
a_2 &= \frac{-1+\beta}{1+\beta} \\
a_3 &= \frac{-D_x(\Delta t)^2}{\rho h(\Delta x)^4} \\
a_4 &= \frac{-D_y(\Delta t)^2}{\rho h(\Delta x)^4} \\
a_5 &= \frac{-D_{xy}(\Delta t)^2}{\rho h(\Delta x)^4} \\
a_6 &= \frac{(\Delta t)^2}{\rho h(\Delta x)^2} \ ,
\end{aligned}
\tag{10}
$$

where we have included a driving force and damping as before.

Some results for $\mid Z \mid$ for a square orthotropic plate are given in Fig. 3. Here we have used a set of elastic constants which have been measured for a real soundboard [5], and which are also close to values given elsewhere in the literature [31]. Other plausible values for the elastic constants yield similar results. Comparing with the experiments in Fig. 1 we find that $\mid Z \mid$ is too small by about a factor of 4 in the range $100 - 10^3$ Hz, implying that our orthotropic model is not stiff enough in this range. In addition, the calculated impedance again varies much too weakly with frequency above $\sim 10^3$ Hz, as it decreases by less than a factor of ~ 2 in going from 10^3 to 10^4 Hz (note that the vertical scale in Fig. 3 spans only one decade, and is thus quite different those in our other impedance plots). The measured impedance drops by a factor of ~ 30 in the same range. This weak frequency dependence of $\mid Z \mid$ should come as no surprise, since for an orthotropic board the density of modes is again independent of frequency at high frequencies [5].

V. ANISOTROPIC BOARD WITH RIBS

The behavior found for the orthotropic board in Fig. 3 indicates that $\mid Z \mid$ is too small at low frequencies. We thus need to make the board stiffer in this frequency range; this can be accomplished by choosing a material with a larger Young's modulus, or employing a thicker board, or both. However, we would still have the problems of too little frequency

dependence from $10^3 - 10^4$ Hz, and an impedance which is too large at high frequencies. We need to devise a way to construct a board which is effectively stiffer at low frequencies (long wavelengths), but is at the same time softer at high frequencies (short wavelengths). From a qualitative standpoint this can be accomplished by adding ribs to the board. Consider ribs that run along the "soft direction," which in our case is y; i.e., across the grain as on a real soundboard. Ribs can increase the stiffness in two ways. First, they can have a larger Young's modulus than the across-the-grain value; that is, $E_{rib} > E_y$. Second, they add thickness to the board thus increasing h, and this increases the rigidity as can be seen from (9). In words, this simply means that a thick board is harder to bend than a thin one, even if E is held fixed. The ribs thus cause long wavelength vibrations to experience a stiffer board. Here "long" means a wavelength comparable to or greater than the rib spacing. On the other hand, vibrations with wavelengths smaller than the rib spacing can effectively fit into the spaces between ribs and thus experience a softer board characteristic of E_y.

These arguments have motivated us to study a model in which ribs are added to the orthotropic board of the previous section [35]. Ours is not the first soundboard model to include ribs, as such a model was also considered by Kindel [4,5]. However, his concern was with the precise eigenfrequencies and eigenvectors of the low frequency modes (generally below a few hundred Hz), whose wavelengths are larger than the rib spacing. He was therefore able to employ a model similar to (8) with suitably chosen, i.e., spatially averaged, values for the rigidities D_x, D_y, and D_{xy}, and other parameters. In this way, he was able to employ an equation of motion similar to (8) which was appropriate (and accurate) for the long wavelength modes which were his primary concern. However, since we are also interested in the short wavelength modes we must explicitly include the position dependences of the elastic constants and board thickness. Our approach is motivated by the finite difference form for the equation of motion (8), which can be interpreted as simply Newton's second law for the mass elements of volume $h(\Delta x)^2$ which make up the board.

We begin with an orthotropic board similar to that treated in the previous section. We then add ribs and let them be evenly spaced and run parallel to the y direction (which

is perpendicular to the direction of the "grain" in the model). The ribs are taken to be narrow, and for simplicity we give them a width of one spatial grid size, Δx. For our typical calculations this corresponds to $1-2$ cm, which is close to the width in a real case [36]. In the regions of the board between the ribs [i.e., for the corresponding values of (i,j)] the equation of motion is the same as (8) with the rigidities given previously (9), since the elastic restoring forces and the geometry of the mass elements are the same as for a board without ribs. For locations on the ribs we *assume* that we can use an equation of motion of the same form, but with several parameters altered due to the different thickness and Young's modulus of the ribs. For the rib locations we take

$$\begin{aligned} D_{x,rib} &= \frac{h^3 E_x}{12(1-\nu_x\nu_y)} \\ D_{y,rib} &= \frac{(h+h_{rib})^3 E_{rib}}{12(1-\nu_x\nu_y)} \\ D_{xy,rib} &= \frac{(h+h_{rib})^3 G_{xy}}{12} \ , \end{aligned} \tag{11}$$

where h_{rib} is the thickness of a rib, and E_{rib} is its Young's modulus (we ignore any anisotropy here). The physical motivation for these expressions for the rigidities can be understood as follows. Since a rib is only one spatial step wide and runs parallel to y, the connection to neighboring parts of the board in the x direction will be the same as if there were no rib present. Hence the resistance to bending in the direction perpendicular to the rib, and thus $D_{x,rib}$, will be the same as without ribs. Things are different along the rib direction, y, as here the rib must bend with the board. For this reason, the rigidity $D_{y,rib}$ is determined by the thickness of the board plus rib, $h+h_{rib}$, and the Young's modulus of the rib, E_{rib} (assumed to be much larger than E_y). For the shear term we have for simplicity assumed that it is the same as without ribs, except that we allow for the thickness of the rib [37]. Finally, we have neglected changes in Poisson's ratio on the ribs, as these have a numerically small effect in (11). Our expressions for the rigidities are at best approximate; in particular, they ignore factors which arise due to the fact that the "neutral surface" of a rib, i.e., the plane through the center of mass of rib is displaced relative to that of the board without

ribs [5]. Including these effects has been shown to alter the form of the equation of motion, although the additional terms appear to be numerically small in our case. In any event, to do a better job would require a more extensive finite element analysis, with much smaller spatial step sizes (much smaller than the rib width). While such an analysis might be warranted (and would be interesting to pursue) in the future, we believe that at this stage a computationally simpler, albeit approximate, approach will yield more physical insight. A similar approach yielding a "practical" theory of the orthotropic plate has been shown to give results close to the exact, and much more involved, theory [7].

Our numerical scheme for a board with ribs may be summarized as follows. At all locations (i, j) we use the finite difference result (5) to compute $z(i, j, n+1)$. For locations (i, j) which are not on a rib we use the coefficients a_i from (10) with the rigidities (9). For locations which are on a rib we use the same form for the a_i coefficients, but with the following changes: the rigidities are taken from (11) and the factors of h which appear explicitly in (10) are replaced by $h + h_{rib}$. The loss factor R is the same as for the off-rib locations.

We have investigated the behavior of our model with ribs for a variety of parameter sets, and the results presented in Fig. 4 are typical. The elastic constants used here are those measured by Kindel for a real soundboard, and which he found to give good agreement with experiment in his model calculations of the low frequency modes for a grand piano. These parameter values are also close to those reported elsewhere in the literature [31]. We have assumed a rib thickness of 1 cm and a Young's modulus of the rib of $E_{rib} = 2 \times 10^{10}$ N/m^2. As one would expect from (11), very similar results are found if the rib thickness is increased and E_{rib} is reduced. The results in Fig. 4 exhibit all of the features that we have argued are musically important. First, the fundamental frequency is near 100 Hz. Second, $\mid Z \mid$ is approximately constant with a value near 10^3 kg/s in the range $100 - 10^3$ Hz. Third, the impedance drops significantly as the frequency increases from 10^3 to 10^4 Hz. All of these features agree at least semiquantitatively with measurements on real soundboards, and they can also be readily understood on a physical basis.

At low frequencies the ribs increase the stiffness of the board in the y direction. This increases the impedance at low frequencies as compared to the orthotropic board without ribs in Fig. 3. For the results shown here we assumed that there are 12 ribs, which seems to be a typical value, and that they are evenly spaced across the board. This rib configuration together with the values used for the rib thickness and Young's modulus given above, resulted in a value of $\mid Z \mid$ at 100 Hz which is quite close to the desired value. Our calculations show that this impedance can be increased by adding more ribs, increasing their thickness, increasing E_{rib}, or any combination of these changes.

For the calculation shown in Fig. 4, the "average" value of the impedance (i.e., the value found after averaging over the resonances) was approximately constant from 100 up to ~ 2000 Hz, and then decreased at higher frequencies. The frequency at which $\mid Z \mid$ began to decrease was found to depend on the number of ribs. As the number of ribs was reduced this frequency dropped, while adding ribs kept $\mid Z \mid$ constant up to a higher frequency. This agrees with the arguments given at the beginning of this section. The ribs increase the stiffness and hence increase $\mid Z \mid$ for wavelengths comparable to or longer than the rib spacing, while allowing the board to be "softer" at shorter length scales. Indeed, we see that the impedance at 10^4 Hz for the board with ribs approaches the value observed for the orthotropic board without ribs, Fig. 3.

The results in Fig. 4 agree fairly well, but not perfectly, with the measured results. The main difference between the two is that the calculated impedance at 10^4 Hz is somewhat larger, here by about a factor of 3–5, larger than the experimental value. This difference could perhaps be eliminated by fine tuning the elastic constants and adjusting the properties of the ribs (their number, spacing, length, and thickness). However, given the approximate nature of our model, we do not consider such "fits" to be warranted at present. It is also interesting to compare our calculations with the measurements of Conklin [19]; as mentioned above, Conklin reported that Z is essentially frequency independent from $1000 - 5000$ Hz. It is seen that the calculated impedance for a board with ribs in Fig. 4 changes only a little over this range, with most of the decrease at higher frequencies. Hence, our calculation

seems consistent with the experiments of both Wogram [13] and Conklin [19]. In any event, it seems safe to conclude that this model contains the ingredients necessary to account for the general behavior observed experimentally.

VI. OTHER SOUNDBOARD PROPERTIES

So far we have focussed our attention entirely on the behavior of $\mid Z \mid$. In this section we will consider two other important properties, the phase associated with the impedance, and the sound production. Results for the phase angle, ϕ, between the driving force and the soundboard velocity are shown in Fig. 5. These results are for the board with ribs considered in Fig. 4. At low frequencies, $f < 100$ Hz, the board velocity is largely out of phase with the driving force, as expected for an oscillator when f is below the frequency of the fundamental mode. In the intermediate range the phase angle approaches zero, as F and v are essentially in phase with each other. Hence, at these frequencies the transfer of energy from the string to the board is fairly efficient. Above about 10^3 Hz the phase angle decreases, as observed experimentally. The overall behavior is in fairly good agreement with the measurements in Fig. 1. The only significant difference appears to be at the highest frequencies, where the calculated phase angle approaches $-90°$ somewhat more slowly than found in the measurements. The reason for this is not completely clear, but it may be due to discreteness effects in our finite element approach (such as taking the ribs to be one spatial unit wide), rather than being inherent in the model.

As we have mentioned several times, one motivation for our work has been the desire to construct a soundboard model which can be used for simulation studies involving string vibrations. The hope is to combine string simulations like those in Refs. [1,2] with our model soundboard; that is, to effectively terminate the strings in the simulations at a point on our model soundboard. This would allow one to investigate the coupling between strings and other related issues. Of course, one goal of such calculations would be to produce a convincing piano sound, and this brings up the question of how to calculate the sound

produced by our theoretical soundboard.

The calculation of the sound produced by a vibrating board is not as straightforward as the calculations of the impedance and phase angle considered above. The usual treatments of sound production by vibrating sources are usually limited to geometrically simple objects, and deal only with the frequency domain, since the propagation problem (in the surrounding medium) is then simpler than when viewed in the time domain [38]. However, our square board with ribs is not a simple source and things will become more complicated when (in the future) we consider more realistic soundboard geometries. We also do not wish to work in the frequency domain, for reasons already mentioned. These considerations lead us to consider two approximate approaches. Our aim here is to judge if either might be adequate for further simulation studies.

In the first approach we assume that each finite difference element of the board contributes to the radiated power independently of all of the other elements, and that the power contributed by an element is proportional to the square of its velocity. With these assumptions the total radiated power is

$$P_1 \sim \sum_{i,j} v(i,j)^2 \ , \tag{12}$$

where $v(i,j)$ is the velocity of element (i,j) and is calculated by averaging the instantaneous board velocity $v(i,j,n+1) = [z(i,j,n+1) - z(i,j,n)]/\Delta t$ over one period of the driving force. This approach ignores the interference of the sound generated by different regions of the board, which leads to a reduction of the radiation efficiency with increasing frequency [16]. We therefore expect that (12) will overestimate the sound level at high frequencies. Even with this significant deficiency (and we should expect other difficulties at low frequencies [38]), it is instructive to consider the behavior of P_1.

In our second approach to the calculation of the radiated sound, we treat the board as effectively a single oscillator and assume that the total radiated power is proportional to the square of the average velocity of the entire board. This approach, which has been used in guitar modeling [10], yields the sound power

$$P_2 \sim \left[\sum_{i,j} v(i,j)\right]^2 \quad . \tag{13}$$

This expression allows in a crude sense for cancellation of sound produced by different regions. Before discussing the behavior of P_1 and P_2 we wish to emphasize that they are only *approximations*. Their ultimate usefulness can only be determined by comparison with a more detailed treatment.

Results for P_1 and P_2 for our soundboard with ribs are shown in Fig. 6. Note that we have followed the experiments [13] and plotted the radiated power for a fixed board velocity (v_0) at the driving point as a function of frequency. The expressions given above for P_1 and P_2 were evaluated by averaging over one complete period of the driving force, after the system had reached a steady state. Approximations P_1 and P_2 both exhibit a rapid increase as f increases from 20 to about 100 Hz. At higher frequencies P_1 is essentially constant up to 10^4 Hz, while P_2 exhibits a maximum at $\sim$ 100 Hz and a rapid decrease at higher frequencies. When comparing with the measurements in Fig. 1 we see that P_1 is much too large at high frequencies; that is, P_1 does not decrease sufficiently (or at all) at high frequencies. This deficiency can be readily understood from the arguments given above. On the other hand, we see that P_2 compares fairly well with the measured result. In particular, the calculated decrease as the frequency varies from a few hundred Hz to 10^4 is about a factor of 10^4, while the observed value is the same to within about a factor of 3. It thus appears that the approximation P_2 may be satisfactory for future simulations.

VII. DISCUSSION

To the best of our knowledge the only experimental results for the impedance and other properties of a piano soundboard over the full "high" frequency range ($10^3 - 10^4$ Hz) are those in Ref. [13]. We have compared our model results to those measurements where possible, and have used what we have argued are the important features of the experimental results for $\mid Z \mid$ to guide us to the model with ribs. The overall agreement is encouraging as our

calculated impedance has the correct overall magnitude and frequency dependence, at least semi-quantitatively. Nevertheless, many refinements of the model are needed. These include the addition of the bridges, allowing motion in all three dimensions, and adding "crown" to the board. Further study of how best to calculate the sound produced by a vibrating soundboard is also needed.

We have argued that the ribs are essential for producing the desired variation of the impedance with frequency. It is interesting to note that Wogram has reported a few results for soundboards without ribs [25]. He measured $\mid Z \mid$ as the ribs were removed in stages by grinding them off an originally complete soundboard. Surprisingly, while removing the ribs in this way did have some effect on the frequencies of the lowest modes, the general behavior of $\mid Z \mid$, even above 10^3 Hz, was essentially the same after the ribs were completely removed. This result runs counter to our arguments. There are two ways to explain this discrepancy. (1) Our arguments are wrong. Obviously, we do not believe that this is the case. If Wogram's results for a soundboard without ribs are really correct, then the impedance of an orthotropic plate should exhibit the features seen in Fig. 1. However, given our calculations for this case we do not see how the impedance of an orthotropic plate without ribs can be made to resemble the measured result. One place for significant maneuvering in our model concerns the loss term. We have employed a very simple and numerically convenient choice for the loss, but one could imagine a rather different possibility. Suppose that the loss is dominated by sound production. We know from the experiments that the efficiency of sound generation drops substantially above 10^3 Hz. This effect could then make the board effectively softer at high frequencies and reduce $\mid Z \mid$. We do not believe that this is a plausible scenario [39,40], but cannot discount it at present. (2) There may be a problem with the experiments. We are reluctant to comment much on this point, but do note that the complete removal of a rib may not be a simple task. If the glue used to attach the ribs to the soundboard had penetrated into the board, which seems likely, this could add extra stiffness even when the rib material itself was completely ground away. This discussion also raises the possibility that the results in Fig. 1 for a soundboard with ribs may need to be reexamined. This possibility

may seem a bit discouraging from the point of view of this paper, since we have made use of trends in the measured impedance in Ref. [13] to lead us to our final soundboard model. However, the key feature we have utilized is the decrease of $\mid Z \mid$ at high frequencies, and we have given arguments independent of the experiments (involving the frequency dependence of the decay rate, as discussed above) that such behavior should be expected [41]. In any event, more experimental work would clearly be desirable.

In summary, we have investigated the properties of a simple finite element model of a piano soundboard, and are encouraged by the level of agreement between our results and experimental measurements. We have argued that ribs are an essential ingredient in obtaining this agreement, but further experiments are needed to determine if this is in fact the case.

We are grateful to P. F. Muzikar and A. J. Korty for useful comments, especially concerning the manuscript, A. Tubis for remarks concerning timpani vibrations, G. Weinreich (and also one of the referees) for some very interesting comments regarding the experimental situation, and B. Martin for inspiring discussions. We are also indebted to H. W. Jackson for providing a copy of Ref. [5]. This work was supported in part by the NSF through grant PHY-9722031.

REFERENCES

[1] A. Chaigne and A. Askenfelt, "Numerical simulations of piano strings. I. "Physical model for a struck string using finite difference methods," J. Acoust. Soc. Am. **95**, 1112 (1994).

[2] A. Chaigne and A. Askenfelt, "Numerical simulations of piano strings. II. Comparisons with measurements and systematic exploration of some hammer-string parameters," J. Acoust. Soc. Am. **95**, 1631 (1994).

[3] I. Nakamura, "The vibrational character of the piano soundboard," Proc. 11th ICA, Paris (1983), Vol. 4, p. 385.

[4] J. Kindel and I-C. Wang, "Modal analysis and finite element analysis of a piano soundboard," in *Proceedings of the 5th International Modal Analysis Conference,* (Union College, Schenectady, New York, 1987), p. 1545.

[5] J. Kindel, "Modal analysis and finite element analysis of a piano soundboard," Masters thesis, University of Cincinnati, 1989.

[6] While not strictly intended to apply to piano soundboards, the work of Ref. [7] on the vibrations of orthotropic plates is also quite relevant to the problems considered in the present paper.

[7] G. W. Caldersmith, "Vibrations of orthotropic rectangular plates," Acustica **56**, 144 (1984); G. Caldersmith and T. D. Rossing, "Determination of modal coupling in vibrating rectangular plates," Appl. Acoustics **17**, 33 (1984).

[8] H. L. Schwab, "Finite element analysis of a guitar soundboard," Catgut Acoust. Soc. **24**, 13 (1975). H. L. Schwab and K. C. Chen, "Finite element analysis of a guitar soundboard - Part II," Catgut Acoust. Soc. **25**, 13 (1976).

[9] O. Christensen and B. B. Vistisen, "Simple model for low-frequency guitar function," J. Acoust. Soc. Am. **68**, 758 (1980).

[10] O. Christensen, "An oscillator model for analysis of guitar sound pressure response," Acustica **54**, 289 (1984).

[11] A. Chaigne, "On the use of finite differences for musical synthesis. Application to plucked string instruments," J. Acoustique **5**, 181 (1992).

[12] See, for example, B. E. Richardson, G. W. Roberts, and G. P. Walker, "Numerical modeling of two violin plates," J. Catgut Acoust. Soc. #47, p. 12 (1987).

[13] K. Wogram, "Acoustical research on pianos. Part I: Vibrational characteristics of the soundboard," Das Musikinstrument **24**, 694 (1980); *ibid* p. 776 and 872.

[14] Note that while Ref. [13] plotted the sound pressure level, we have chosen here to plot the sound power level. This affects the vertical scale, but not the overall shape of this $\log - \log$ plot.

[15] H. Suzuki, "Vibration and sound radiation of a piano soundboard," J. Acoust. Soc. Am. **80**, 1573 (1986).

[16] N. H. Fletcher and T. D. Rossing, *The Physics of Musical Instruments,* (Springer-Verlag, New York, 1991).

[17] A. H. Benade, *Fundamentals of Musical Acoustics* (Oxford University Press, New York, 1976).

[18] G. Weinreich, "Coupled piano strings," J. Acoust. Soc. Am. **62**, 1474 (1977).

[19] H. A. Conklin, Jr., "Design and tone in the mechanoacoustic piano. Part II. Piano structure," J. Acoust. Soc. Am. **100**, 695 (1996).

[20] The frequency at which this fall off begins depends somewhat on the position on the soundboard where the impedance is measured, and was observed [13] to vary by a factor of ~ 2. However, above this point $\mid Z \mid$ decreased at approximately the same rate with frequency at all locations on the soundboard.

[21] D. W. Martin, "Decay rates of piano tones," J. Acoust. Soc. Am. **19**, 535 (1947).

[22] T. C. Hundley, H. Benioff, and D. W. Martin, "Factors contributing to the multiple rate of piano tone decay," J. Acoust. Soc. Am. **64**, 1303 (1978).

[23] We should also note that Ref. [19] has shown the results of impedance measurements which do not show any significant decrease in the impedance at high frequencies. However, those results extend to only about 5000 Hz, so they may be consistent with those of Wogram [13]. In any event, it would be very desirable to reexamine the experimental situation, as will be discussed further below.

[24] Conklin [19] gives a particularly instructive discussion of soundboard design and behavior.

[25] K. Wogram, in *The Acoustics of the Piano*, Royal Swedish Academy of Music Publication No. 64 (Stockholm, 1990), edited by A. Askenfelt, p. 83.

[26] L. D. Landau and E. M. Lifshitz, *Theory of Elasticity* (Pergammon, London, 1959).

[27] There is a substantial literature (see, for example, Ref. [28] and references contained therein) on the vibrations of plates whose thickness varies with position, since structures of this type serve many practical functions. In most cases the analysis of such stepped plates, which are similar in some respects to the model with ribs which we will discuss below, is limited to plates with a single step. Additional steps can be accommodated within the theory, but only with significant computational complications which end up making the problem essentially a numerical one. Given our ultimate goal of modeling a semi-realistic soundboard, it therefore seems reasonable to take a numerical approach from the outset.

[28] I. E. Harik, X. Liu, and N. Balakrishnan, "Analytic solution to free vibration of rectangular plates," J. Sound and Vib. **153**, 51 (1992).

[29] N. Giordano, *Computational Physics* (Prentice Hall, Upper Saddle River, NJ, 1997).

[30] Other details of the calculation, such as the choice of time step, etc., follow standard practice, as discussed in Refs. [29,11,1].

[31] V. Bucur, *Acoustics of Wood,* (CRC Press, Boca Raton, 1995).

[32] L. Cremer and M. Heckl, *Structure-Borne Sound* (Springer-Verlag, New York, 1973).

[33] For most upright pianos, including the one studied in Ref. [13] for which schematic results are given in Fig. 1, the grain of the soundboard runs diagonally, rather than parallel to one of the edges as we assume here. This is one of the details that we will assume can be neglected in a "first" approximation.

[34] S. G. Lekhnitskii, *Anisotropic Plates* (Gordon and Breach, New York, 1968).

[35] For simplicity we will not include the bridges in our model. Since the bridges generally run approximately parallel to the stiff direction (in our case x), we expect that they will affect the behavior much less than the ribs.

[36] Ideally one would like to have the spatial step size in a calculation be much smaller than any of the important length scales in the problem. However, using a significantly smaller value of Δx would add greatly to the computational demands, but not, we think, much to the physical insight.

[37] Our approach is in the same spirit as the approximate theory for orthotropic plates developed in Ref. [7], where it was shown that in practice, accurate results are obtained if the shear modulus is chosen such that $D_{xy} = \sqrt{D_x D_y}$. Our choice of G_{xy} here and above satisfies this criterion to within 20% or better. Variations of the value of G_{xy} by this amount did not have a significant effect on the results.

[38] P. M. Morse and K. U. Ingard, *Theoretical Acoustics* (Princeton University Press, Princeton, 1986).

[39] It is known from Ref. [40] that air loading has a quite significant effect on the modes of

a timpani membrane. However, given its different thickness and mass density, we would not expect air loading to be nearly as important for a piano soundboard.

[40] R. S. Christian, R. E. Davis, A. Tubis, C. A. Anderson, R. I. Mills, and T. D. Rossing, "Effects of air loading on timpani membrane vibrations," J. Acoust. Soc. Am. **76**, 1336 (1984).

[41] It has been pointed out by G. Weinreich (private communication) that other factors connected with the decreasing length of the strings may also play a major role in producing faster decays at high frequencies. This would appear to be a (currently unsettled) question which requires more experimental work.

FIGURES

FIG. 1. Schematic soundboard properties after the results given in Ref. [13] for an upright piano. Top: magnitude of the mechanical impedance; middle: sound power level [14]; bottom: phase of the soundboard velocity relative to the phase of the driving force. The resonant structure due to a few of the lowest modes is shown. The results were obtained by exciting the board at a point on the treble bridge near the center of the soundboard, and the velocity was measured at the driving point (the results for other excitation points were similar). Note that the result for the sound level was obtained with a constant velocity at the driving point.

FIG. 2. Calculated driving point impedance for an elastically isotropic board. The board was 1×1 m^2, and the spatial step size used in the calculation was $\Delta x = 0.02$ m, and the loss factor was $R = 1$ kg/(m^2 – s). Filled circles: $E = 1 \times 10^{10}$ N/m^2, $\nu = 0.3$. Open circles: $E = 4 \times 10^8$ N/m^2, $\nu = 0.3$. The driving point was at $x = y = 0.3$ m, with the origin at one corner of the board.

FIG. 3. Calculated driving point impedance for an orthotropic (anisotropic) board. Values of the elastic constants appropriate for spruce were used: $E_x = 1 \times 10^{10}$ N/m^2, $E_y = 4 \times 10^8$ N/m^2, $G = 1 \times 10^9$ N/m^2, $\nu_x = 0.4$, and $\nu_y = 0.01$. The other parameters were the same as in Fig. 2.

FIG. 4. Calculated driving point impedance for an orthotropic (anisotropic) board with ribs. The elastic constants were the same as those used in Fig. 3. We also took $h_{rib} = 0.01$ m and $E_{rib} = 2 \times 10^{10}$ N/m^2. The board had 12 evenly spaced ribs.

FIG. 5. Calculated phase angle between the driving force and the soundboard velocity for the soundboard with ribs considered in Fig. 4.

FIG. 6. Calculated sound production for the soundboard with ribs considered in Fig. 4, using the approximations (12) and (13). Note that the vertical scales are arbitrary, and are not the same in the two cases.

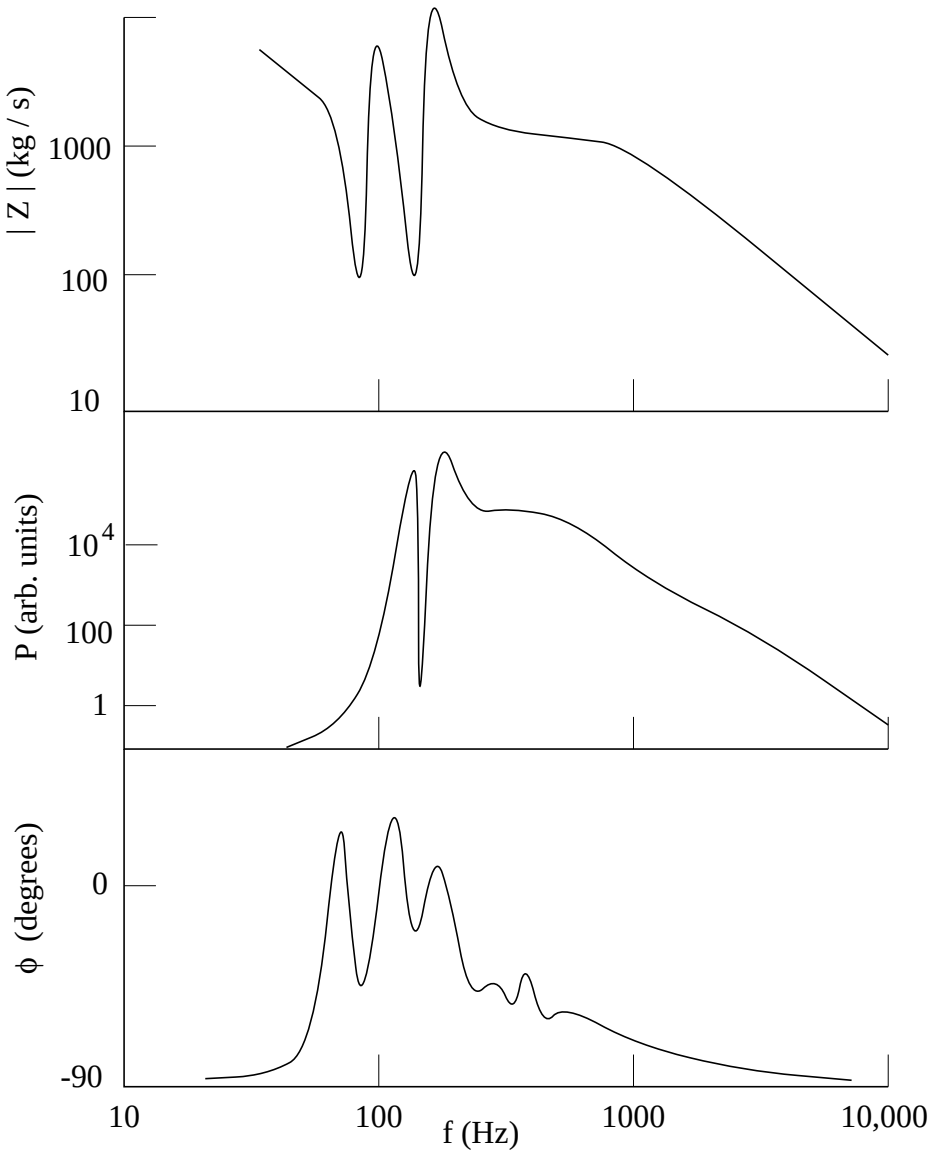
| Z | (kg / s)
1000
100
10
P (arb. units)
10^4
100
1
ϕ (degrees)
0
-90
10
100
1000
10,000
f (Hz)

Figure 1

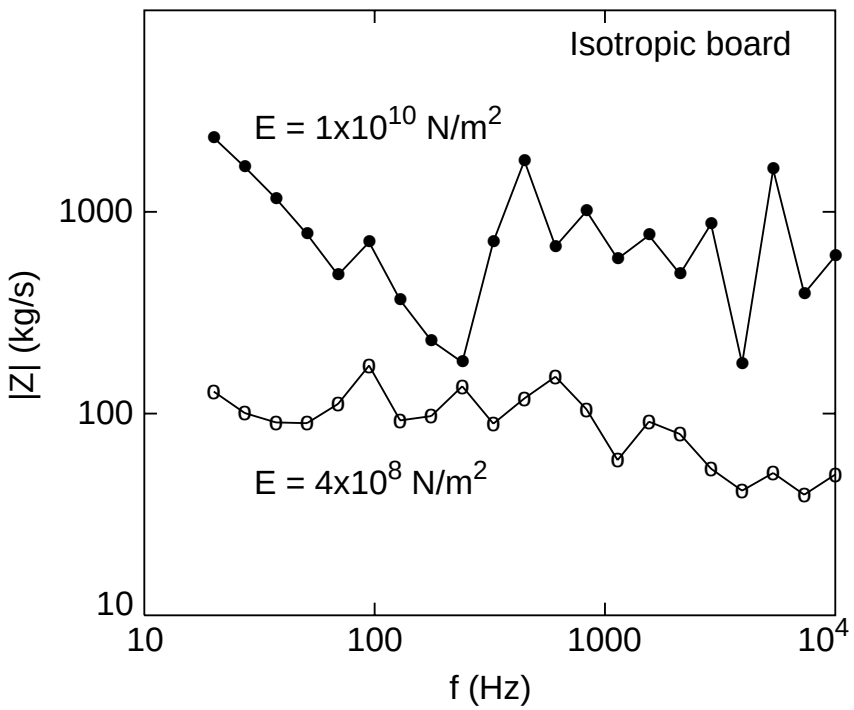
Isotropic board
E = 1x10^10 N/m^2
E = 4x10^8 N/m^2
|Z| (kg/s)
1000
100
10
10
100
1000
10^4
f (Hz)

Figure 2

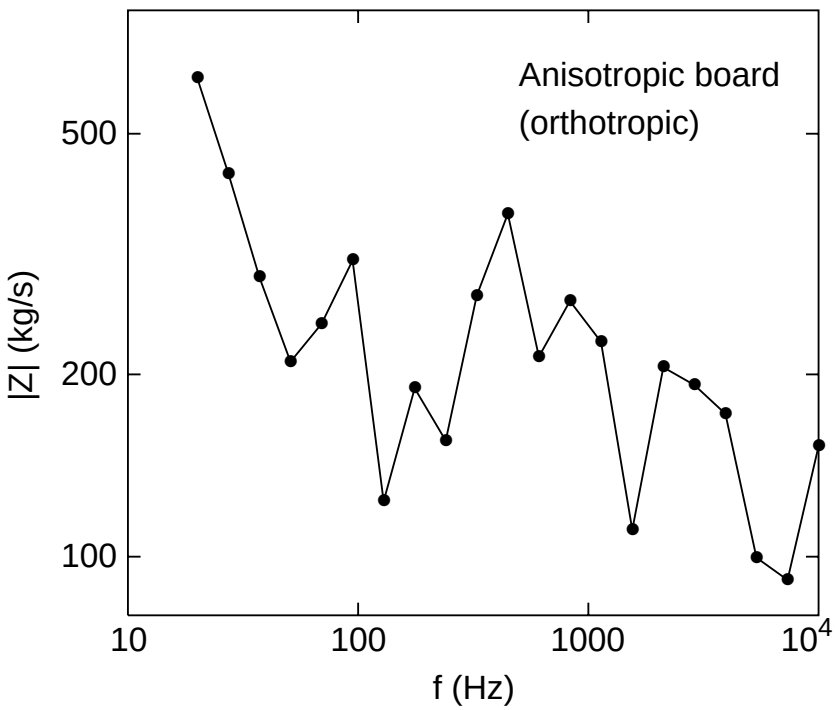
Anisotropic board
(orthotropic)
500
200
100
|Z| (kg/s)
10
100
1000
10^4
f (Hz)

Figure 3

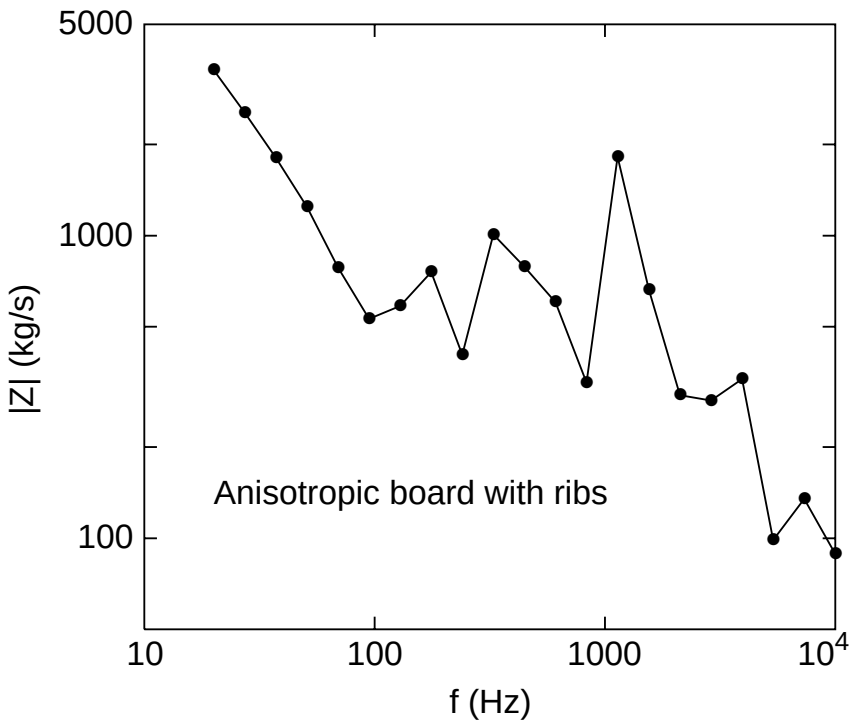

Figure 4

(Giordano)

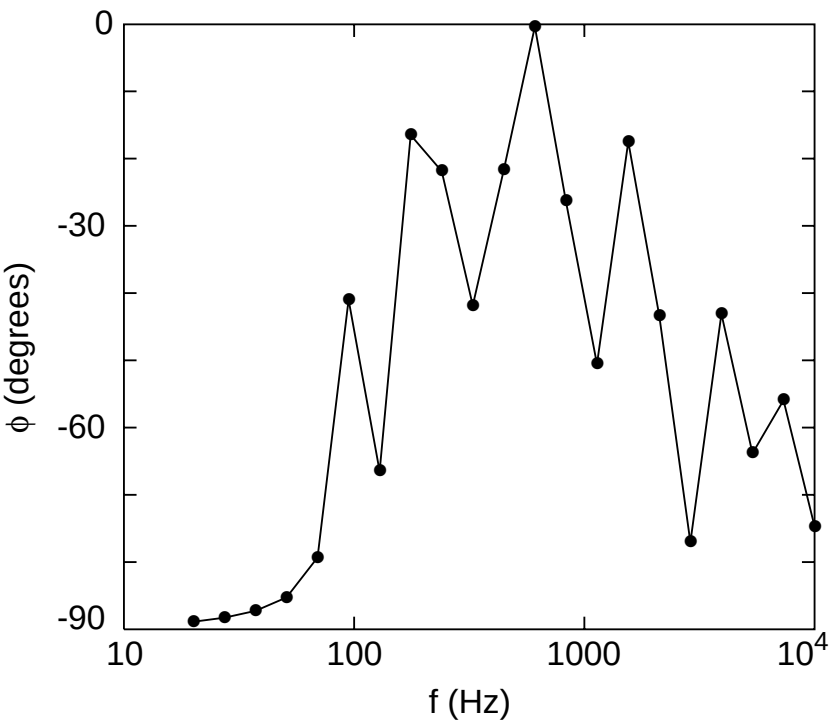

Figure 5

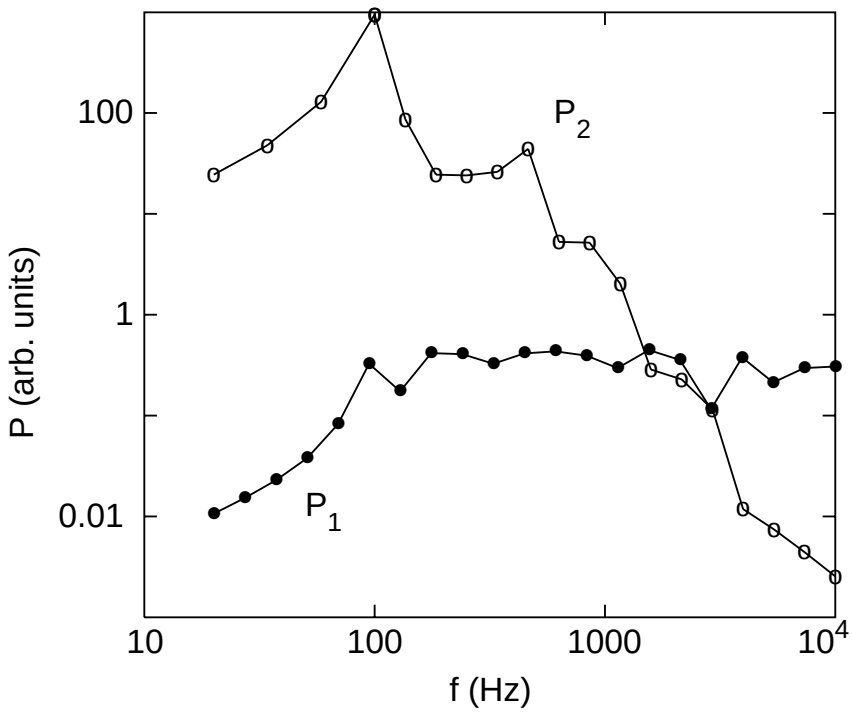

Figure 6